Rolled-up transparent microtubes as two-dimensionally confined culture scaffolds of individual yeast cells

Gaoshan Huang,* Yongfeng Mei,* Dominic J. Thurmer, Emica Coric and Oliver G. Schmidt

Received 19th June 2008, Accepted 19th August 2008
First published as an Advance Article on the web 23rd October 2008
DOI: 10.1039/b810419k

Transparent oxide rolled-up microtube arrays were constructed on Si substrates by the deposition of a pre-stressed oxide layer on a patterned photoresist sacrificial layer and the subsequent removal of this sacrificial layer. These microtubes as well as their arrays can be well positioned onto a chip for further applications, while their dimensions (e.g. length, diameter and wall thickness) are controlled by tunable parameters of the fabrication process. Due to the unique tubular structure and optical transparency, such rolled-up microtubes can serve as well-defined two-dimensionally (2D) confined cell culture scaffolds. In our experiments, yeast cells exhibit different growth behaviors (i.e. their arrangement) in microtubes with varied diameters. In an extremely small microtube the yeast cell becomes highly elongated during growth but still survives. Detailed investigations on the behavior of individual yeast cells in a single microtube are carried out *in situ* to elucidate the mechanical interaction between microtubes and the 2D confined cells. The confinement of tubular channels causes the rotation of cell pairs, which is more pronounced in smaller microtubes, leading to different cellular assemblies. Our work demonstrates good capability of rolled-up microtubes for manipulating individual and definite cells, which promises high potential in lab-on-a-chip applications, for example as a bio-analytic system for individual cells if integrated with sensor functionalities.

Introduction

The control and manipulation of living cells by using novel micro- or nanostructures is of great importance in tissue engineering, cancer therapy and fundamental cellular research.[1,2] Various methods and structures have been adopted to control and guide the growth of living cells, such as micropattern arrays,[3] microgrooves[4] and cell adhesion activated by fluorescence.[5] However, these methods merely provide the cell control on a two-dimensional (2D) planar surface. In practice, cells are sensitive, and respond to cues from the environment, and thus behave differently in 2D and 3D,[6] which causes the cell response *in vivo* to vary from that of cells cultured on a 2D flat surface.[7–9] For example, Li *et al.*[8] reported that neuroblastoma cells cultured in a 3D matrix could exhibit differential gene expression and longer neurites than 2D counterparts. Furthermore, traditional biological assays normally analyze the data averaged across large number of cells, and overlook the interesting and valuable information which can be obtained from individual cells.[10–12] Therefore, in order to investigate cell behaviors individually, a 3D micro- or nano-scaffold, which can be employed as an artificial *in vivo* environment, is highly sought-after.[13,14]

Among all 3D microstructures possible for cell culturing, microtubes, which can be also considered as an *in vitro* mimic of a vessel,[15] offer the advantage of a uniform diameter, a good directionality and a strict 2D confinement. Thus, researchers can conveniently use microtubes to practically guide *in vitro* growth of living cells within, and further investigate the mechanical interaction between cells and microtubes. This should be of biological importance because the mechanical interaction between cells and their environment has been previously demonstrated to influence the cellular viability, function and gene expression by inducing cell deformation.[16] In particular, gene expression of budding yeast affected by an external stress has been studied.[17] Although some research has attempted to mimic a 3D environment for tissue engineering by designing well-defined architectures,[18] only a few works have been reported by using microtubular structures as the cell culture scaffolds.[9] We believe this deficiency is mainly due to the lack of an efficient technology for the mass production of microtubular structures with a size similar to the cells, which can be achieved by the rolled-up nanotechnology developed recently.[19,20] The general strategy involves depositing a pre-stressed active layer on a sacrificial layer and then selectively etching away the underlying sacrificial layer to release the active layer which can bend up and eventually roll up into a microtube. Such a universal strategy has been successfully employed to fabricate on-chip-positioned microtubes of various materials and of defined lengths and diameters.[20–22] The successful demonstration of a fluidic application using a microtube[22] also makes rolled-up microtubes suitable candidates for potential applications such as cell culture scaffolds in biological experiments.[12,23–25]

In this work, rolled-up transparent oxide microtube arrays were fabricated and used as 2D confined cell culture scaffolds for individual yeast cells, which could be a useful alternative to animal and mammalian cells.[26] It is worth noting that the high-density microtube array is also relevant for high-throughput cell

Institute for Integrative Nanosciences, IFW Dresden, Helmholtzstr. 20, D-01069 Dresden, Germany. E-mail: g.huang@ifw-dresden.de; y.mei@ifw-dresden.de

assays.[27] These oxide microtubes provide an optically transparent container and enables *in situ* monitoring of the growth and budding of individual yeast cells by optical microscopy. The experimental results indicate that the growth of yeast cells in microtubes can be aligned due to the confinement provided by the tubular channels. Detailed analysis was carried out on the budding of individual yeast cells inside a single microtube to clarify the mechanical interaction between microtubes and yeast cells. This work can pave the way for further explorations of bio-applications of rolled-up microtubes like cell diagnosis employing individual cell arrays.[28]

Experimental

The formation process of rolled-up microtubes is schematically displayed in Fig. 1(a). Briefly, a uniform ARP-3510 photoresist (Allresist GmbH) layer is deposited on a Si (100) wafer by spin-coating at a speed of 3500 RPM. The photoresist patterns with different sizes and shapes (such as squares and circles) are fabricated by using conventional photolithography. The thickness of the obtained photoresist pattern is measured to be ~2 μm by a profiler, and this patterned layer was used as a sacrificial layer in the roll-up process. The active layer (SiO/SiO_2 bi-layer structure) was deposited under high vacuum (< 10^{-4} Pa) by electron beam evaporation with a glancing angle of 75°. The glancing angle deposition adopted in the current experiment

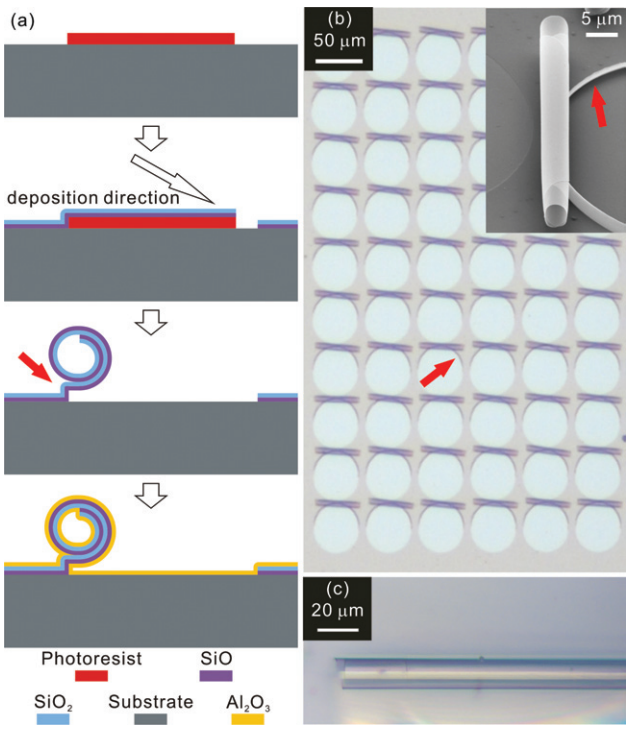

Fig. 1 (a) Schematic diagram illustrating the fabrication process of rolled-up transparent microtubes. (b) Optical microscope image of an ordered array of rolled-up microtubes. The transparent microtubes exhibit excellent alignment and uniformity. The inset shows an SEM image of a typical microtube. The microtube is tightly rolled and a vertical residual film remains. (c) Optical microscope image of a large microtube after Al_2O_3 deposition, where the tube wall remains transparent.

ensures the opening of windows for the following chemical etching process because a gap remains open at the far end of the photoresist pattern due to the ballistic shadow effect in glancing angle deposition (see Fig. 1(a)). This mechanism allows to precisely position the obtained microtubes on the surface and is therefore easily integrated on a chip with different functions. The underetching process was conducted by placing the samples in the chamber of a critical point dryer (CPD030, Bal-Tec AG), which was filled with acetone (Basf GmbH). The acetone can penetrate through the open gap and selectively removes the underneath photoresist layer to release the top active layer. Due to the existence of intrinsic stress in the SiO/SiO_2 bi-layer structure, the free-standing films bend up and self-assemble into a tubular structure. The microtubes were dried in the critical point dryer by using liquid CO_2 as intermedia to avoid collapse. To strengthen the obtained microtubes mechanically, a 50-nm-thick Al_2O_3 layer was deposited onto both the inner and outer surfaces of the microtubes by atomic layer deposition (ALD, Savannah™ 100, Cambridge NanoTech Inc.) prior to cell culture experiments. The treated microtube is robust enough to withstand repeated washing. Besides, the ALD treatment can also improve the bio-compatibility of the tube surface[29,30] and fix the microtubes on a chip more rigidly, which in turn simplifies observation of individual yeast cells (see Fig. 1(a)). In the culture experiment, budding yeast cells (bakery yeast) are used. The chips with different microtubes were put into 50 mL YPD medium (Casein, enzymatically digested 20 g l^{-1}, Yeast extract 10 g l^{-1}, Glucose 20 g l^{-1}, pH-value 6.5 ± 0.2, Carl Roth GmbH + Co. KG) containing yeast cells and cultured overnight at 28 °C. Yeast cells that grew into the microtubes were then used for further characterizations and culturing. The microtube morphology and yeast cell activities were investigated using a combination of scanning electron microscopy (SEM, in Zeiss NVision40 workstation) and optical microscopy (Zeiss Axiotech vario) connected to a camera (Zeiss AxioCam MR) for high-resolution color images.

Results and discussion

Fig. 1(b) shows an optical microscope image of a silicon oxide microtube array formed on circular photoresist patterns (without the additional Al_2O_3 layer). One can see that the transparent oxide microtubes arrange in a highly ordered manner and align into the same direction. This uniform arrangement is controlled by the aforementioned glancing angle deposition, in which the deposition direction and the flux of evaporated materials are the same for all individual photoresist patterns. After chemical etching of the photoresist sacrificial layer, each circularly shaped active layer has rolled up into a microtube, starting from the opening formed at the far side and ending at the opposite well-attached edge of the photoresist layer (Fig. 1(a)), leaving a circular blank area on the substrate. The vertical residual film (see the red arrows in Figs. 1(a) and (b)), which is located at the upper semicircular edge of the blank area, forms during deposition and still partially connects to the tube wall (see enlarged SEM image in the inset of Fig. 1(b)). The height of the vertical film is equal to the thickness of the patterned photoresist layer, which is confirmed by the SEM image. Since the roll-up process will stop automatically at the edge of the photoresist pattern, we

can easily position the microtubes on a chip by designing appropriate geometrical patterns. As one can see in Fig. 1(b), a highly ordered microtube array was formed on circular photoresist patterns having diameters of $D = 40$ μm. The tube diameter d is measured to be ~5 μm (see enlarged SEM image in the inset of Fig. 1(b)). Assuming that the microtube is tightly rolled with compact windings as displayed in the SEM image, we can calculate the maximum rotations n_{max} at the middle part of the microtube by $n_{max} = D/(\pi d)$, which yields ~2.5 rotations in the present case. Geometrical parameters of the obtained microtube such as lengths (from 10 to 1000 μm in current experiment) and rotations can be determined by predefining the photoresist patterns. Therefore, conventional and highly parallel photolithography is a convenient and straightforward way to integrate rolled-up microtubes with different dimensions onto a single chip.

However, the tube diameter cannot be pre-determined by the pattern. It has been shown previously that the diameter of the microtube is influenced by intrinsic stress and structural properties of the active layer.[19,31,32] In microtubes formed from epitaxial bi-layer structures, the intrinsic stress originates from the lattice mismatch, because the materials in the two layers tend to relax toward their bulk lattice constants after being released from the sacrificial layer. Due to the different deposition technique applied here, we consider other mechanisms to explain the existence of the intrinsic stress gradients in our films: firstly, during evaporation different thermal expansions between photoresist layer and active layer could lead to stresses in both layers (there is an increase of the temperature due to the material beam impinging onto the substrate); secondly, varying deposition parameters (e.g. deposition rate) during the active layer deposition can further generate a stress difference. The combination of these two factors introduces an intrinsic stress gradient that causes the bending or rolling of the active layer after release. Although a quantitative explanation of the intrinsic stress in such non-epitaxial layers is still challenging, we are able to control the tube diameter (from ~1.5 to ~14 μm for silicon oxide microtubes) by adopting different experiment parameters. In Fig. 1(c), we show an optical microscope image of a large microtube with a diameter of ~10 μm (compared to the 5 μm diameter in Fig. 1(a)) after coating with a 50-nm-thick Al_2O_3 layer. The microtube is straight and uniform in diameter and still transparent after Al_2O_3 coating.

As for bio-applications of rolled-up microtubes, we first investigate the reproduction of yeast cells in the confinement of a microtube. In this experiment, we cultured the yeast cells in a large microtube with diameter of ~9 μm and length > 600 μm for a duration of 120 min. In order to compare activities of the cells confined in the microtubes to those in a free environment, we also seeded some yeast cells in the free area close to the microtube to ensure the same culture condition. The obtained results about the reproduction of yeast cells are summarized in Fig. 2. Figs. 2(a) and 2(b) display the corresponding optical microscope images of the same region at the beginning (0 min) and the end (120 min) of the culture experiment, respectively. At 0 min, the yeast cells outside the microtube rest sparsely on the flat surface, exhibiting an elliptic geometry. Meanwhile, several yeast cells distribute randomly inside the microtube, and the space between yeast cells is clearly seen. After 120 min of

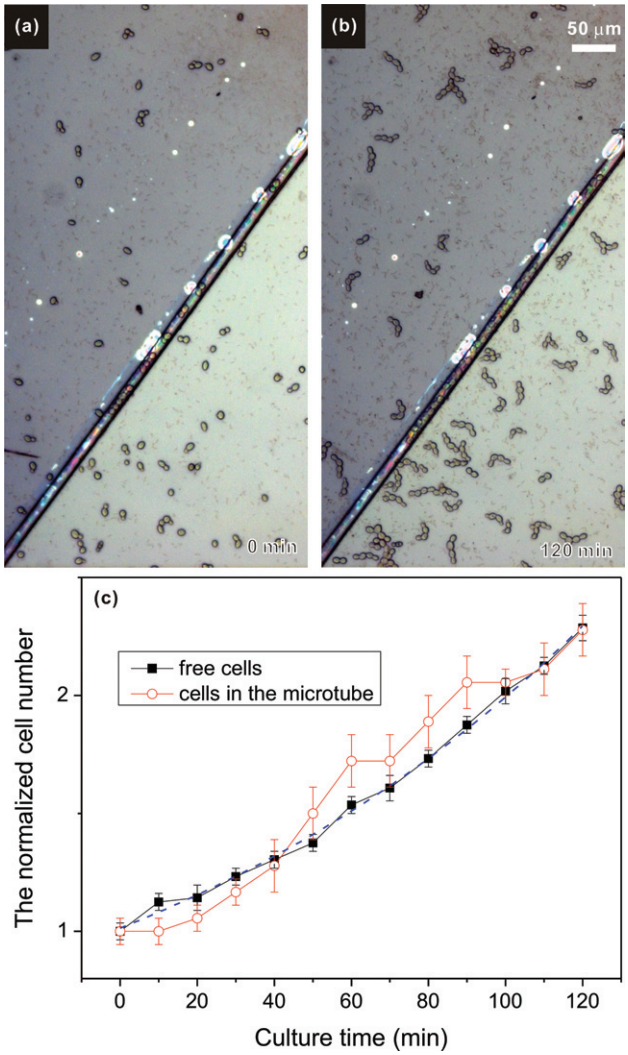

Fig. 2 Optical microscope images of yeast cells inside and outside the microtube after cell culture of (a) 0 and (b) 120 min. The two optical microscope images are obtained at the same region. (c) The normalized cell number as a function of culture time. The black and red plots correspond to cells in free environment and microtube respectively, and no difference between two plots can be observed from a statistical point of view. The blue dashed line shows an exponential fit for growth curve of free cells.

culturing, many yeast cells reproduce by budding. In Fig. 2(b), we can see that the outside yeast cells grow into a dendritic shape through continuous budding. But for the yeast cells inside the microtube, the situation is different. Although the size and shape of the cells do not change significantly, the microtube becomes blocked by new yeast cells due to the space confinement. As a result the yeast cells inside the microtube arrange themselves into a 'zigzag' pattern rather than into the dendritic pattern observed outside the microtube. Quantitatively, we counted and plotted the number of yeast cells as a function of culture time (see Fig. 2(c)). The numbers of the yeast cells inside and outside the microtube are both normalized to 1 at 0 min for the sake of clarity. The reproduction behaviour is similar in both cases and the derived doubling time (~100 min) is similar to the value reported in the literature.[33,34] In addition, we should stress that

the cell density in the microtube ($\sim 1.4 \times 10^4$ mm^{-2}) is much higher than that in the free environment ($\sim 1.3 \times 10^3$ mm^{-2}) after 120 min. Within the chosen time interval, we do not observe any saturation behaviour of the growth rate. This indicates that rolled-up microtubes are bio-compatible and suitable for various bio-applications such as 2D confined cell culture scaffolds. Surprisingly, yeast cells inside this large microtube can obtain enough nutrition for their bio-activities indicating effective transportation and exchange of chemicals through the microtube.

Since the yeast cells in a microtube exhibit an arrangement different from those in a free environment, we tried to use rolled-up microtubes with varying diameters as culture scaffolds for the cell reproduction. Our experimental results demonstrate distinct differences in cell arrangements as microtubes scale down in diameter. Fig. 3(a) displays optical microscope images of 4 different microtubes containing yeast cells after a long-time ($\sim$15 h) culture. The tube diameter was decreased stepwise from left to right (marked by a grey arrow). The microtube in the first panel has the largest diameter of $\sim$14 μm, and the elliptic yeast cells in this microtube arrange into two separated rows. If the tube diameter decreases to $\sim$10 μm, a "zigzag" cell chain is observed in the second panel. This is a similar situation to that in Fig. 2(b). If the tube diameter is further reduced to a value similar to the minor axis of the elliptical yeast cell ($\sim$6.5 μm), the limited space in the microtube only allows the yeast cells to form a single straight row (the third panel). In the fourth panel, a microtube with a smaller diameter ($\sim$5.5 μm) is shown. The yeast cells can migrate into this microtube and are well aligned like a chain but their elongation is clearly seen.

It is quite interesting that yeast cells can reside in an extremely small microtube with a diameter of $\sim$3.5 μm, as demonstrated in Fig. 3(b). Since the tube diameter is much smaller than that of the yeast cell, the yeast cell is assumed to have entered the microtube as a bud. This is strengthened by the observation of its growth with increasing culture time. The volume of this yeast cell increases from $\sim$75 μm^3 at 0 min to $\sim$125 μm^3 at 120 min, indicating the yeast cell is still premature at the beginning of the culture experiment. However, the volume of a typical yeast cell in free environment is $\sim$250 μm^3. Since no further volume expansion of this confined yeast cell was observed with a prolonged culture, the relatively small volume could be ascribed to a nutrition shortage. The height to width aspect ratio of the yeast cells increases from 2.2 to 3.7 after 120 min of culture (see Fig. 3(b)). This value is significantly larger than $\sim$1.3 for a yeast cell in a free environment. In this case, most of the cell wall is tightly pressed against the inner surface of the microtube rather than exposed to the culture media. As a result, although this yeast cell is still alive, the bio-activities are suppressed, leading to a reduced cell volume.

To understand the cell arrangement in more detail, we carried out *in situ* observations of yeast cells growing in the microtubes with diameters of about 9, 6 and 4 μm. The growth and reproduction of yeast cells can be well confined by rolled-up microtubes. The yeast cell pairs (mother cells and their buds) become partially or totally aligned by the microtubes during growth due to the limited free space. We use the angle between the cell pair axis and the tube axis (see insets of Fig. 4) to quantify the

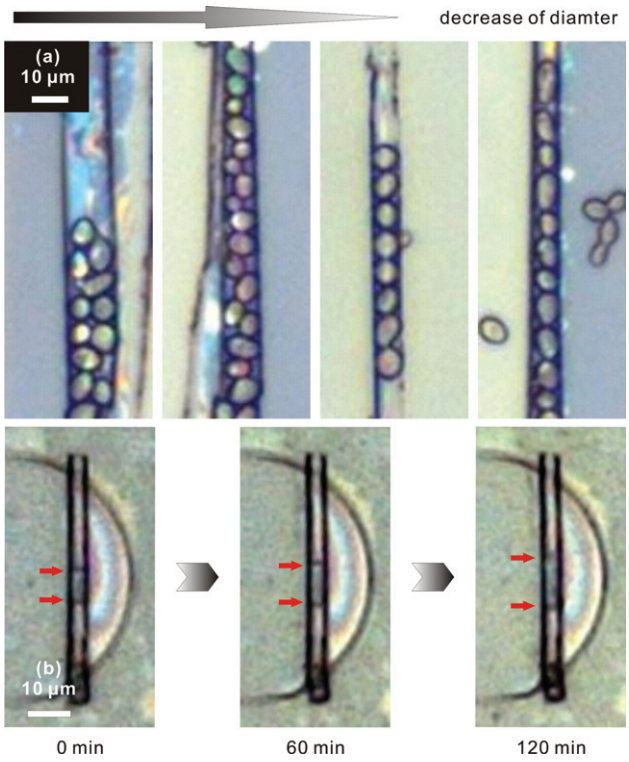

Fig. 3 (a) Optical microscope images of four different microtubes containing yeast cells and the tube diameter was decreased stepwise from left to right. The yeast cells in these microtubes exhibit different arrangements. (b) Optical microscope image of a yeast cell residing in an extremely small microtube. Its aspect ratio can reach 3.7 after a 120-min culture. The red arrows mark the size of the inside yeast cell.

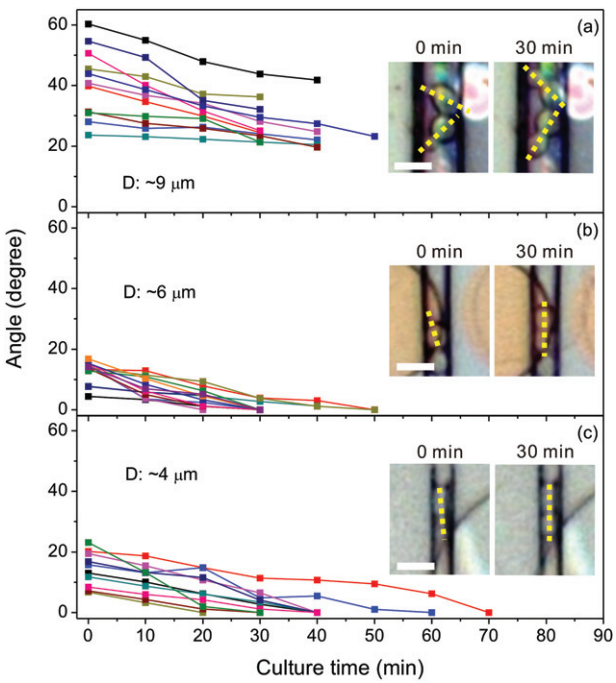

Fig. 4 Evolution of the angle between cell pair axis and tube axis as a function of culture time, using microtubes with different diameters: (a) 9, (b) 6 and (c) 4 μm. Each plot with separated color corresponds to one cell pair. The insets present optical microscope images illustrating the rotation of typical cell pairs with increasing culture time. Scale bar: 10 μm.

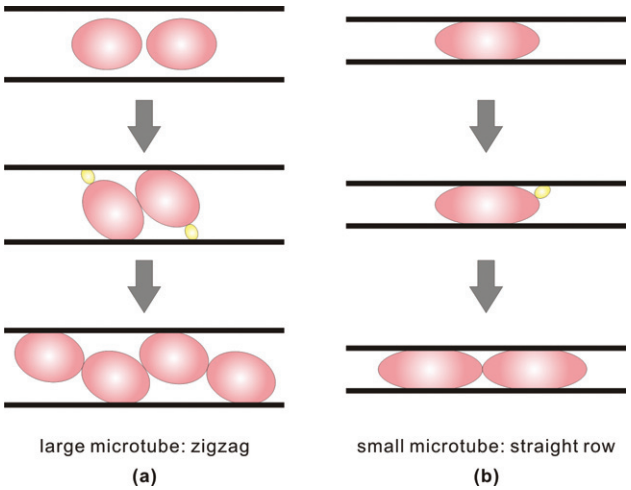

Fig. 5 Schematic diagrams explaining different arrangements of yeast cells in (a) a large microtube and (b) a small microtube.

alignment process of the cells. The plots in Fig. 4 present the angle evolution as a function of culture time for cell pairs in different microtubes. Each plot with separated color corresponds to one individual cell pair. If the tube diameter is larger than the cell (Fig. 4(a), d: ~9 μm), the yeast cells will be pushed together during their budding. Since the microtube used here is relatively large, the mother cell itself can rotate to efficiently use the space for its bud as shown in Fig. 5(a), and the maximum value of the rotating angle increases to more than 60°. However, with the growth of the daughter cell, the confinement of the tubular channels causes a rotation of the cell pair and thus the angle decreases. On the other hand, if the tube diameter is similar to or even smaller than the cell size, the mother cell is well confined and parallel to the tube axis before budding (Fig. 5(b)). According to previous literature,[35,36] the budding sites are always near the tip region of the mother cell. Hence, the initial value of the angle is much smaller in this case than that in the first case, as we can see in Figs. 4(b) and (c) and Table 1. With the growth of daughter cells, the interaction between the tube wall and the daughter cell will drive the daughter cell to the center of the microtube (see Fig. 5(b)). As we can see in Figs. 4(b) and (c), the angle eventually decreases to 0, which is not observed in large microtubes. Here another interesting phenomenon is observed. In Table 1, one can see that the rotation rate is statistically lower for the cell pairs in the culture experiment with the smaller microtubes. This most likely originates from the prominent confinement of the smaller microtube, which hinders the rotation of cell pairs because the yeast cells become more immobile and cannot rotate as easily any more. In addition, since the confinement of smaller microtubes may cause a lack in nutrition, the contained yeast cells are expected to grow at a slower rate, leading to a lower rotation rate.3

Table 1 Statistics about the angle between the cell pair axis and the tube axis. Average starting angle, average ending angle and average rotation rate are calculated for culture experiments in different microtubes. Original data are derived from Fig. 4.

Tube diameter (μm)	Starting angle (degree)	Ending angle (degree)	Rotation rate (degree/min)
9	40.8 ± 11.6	26.5 ± 7.2	0.42 ± 0.23
6	12.7 ± 3.7	0.1 ± 0.4	0.40 ± 0.17
4	14.2 ± 5.8	0	0.37 ± 0.17

Conclusions

We have constructed transparent silicon oxide microtube arrays *via* the rolled-up process which involves conventional photolithography technology, electron beam deposition as well as chemical etching. The microtubes can be well positioned on the substrate and the size tuning is easily realized by altering the geometry of photoresist patterns and deposition parameters. Compared to PDMS technology, the rolled-up technology can fabricate microtubes with a smooth inner/outer surface and a perfect circular cross-section, which could be challenging to achieve for PDMS-based technology. Furthermore, the rolled-up technology can be applied to many materials and material combinations and thus it is relatively easy to fabricate microtubes (microchannels) with customized surface chemical properties provided by the appropriate rolled-up materials.

To explore the feasibility for bio-applications of this kind of rolled-up microtubes, we probed them as 3D cell culture scaffolds which provide a 2D confinement for individual yeast cells inside the microtube. The experimental results demonstrate a good bio-compatibility of rolled-up microtubes. In addition, yeast cells exhibit different arrangements in microtubes with various diameters, which were investigated by *in situ* observation of individual yeast cells, and we found that the confinement of tubular channels caused a rotation of cell pairs. The technology presented in this work provides a possibility for microtubes to integrate functionality as bio-analytic tubular microchannels in lab-on-a-chip applications. For instance, rolled-up microtubes as optical ring resonators,[37] could serve as optofluidic sensors to detect the presence of individual cells inside or even macromolecules involved in their bioactivities, by checking spectral shifts of the optical resonant modes.[38]

Acknowledgements

We are grateful for experimental help by Esteban Bermúdez Ureña, Alexander Solovev, Ronny Engelhard, Barbara Eichler, Sandra Sieber, Dr. Ingolf Mönch and Dr. Jill S. Becker, and helpful discussions with Xiaoxia Pan and Christine Schmidt.

References

1 M. A. Nandkumar, M. Yamato, A. Kushida, C. Konno, M. Hirose, A. Kikuchi and T. Okano, *Biomaterials*, 2002, **23**, 1121–1130.
2 M. Kato and M. Mrksich, *Biochemistry*, 2004, **43**, 2699–2707.
3 G. Kumar, C. C. Ho and C. C. Co, *Adv. Mater.*, 2007, **19**, 1084–1090.
4 R. Kemkemer, S. Jungbauer, D. Kaufmann and H. Gruler, *Biophys. J.*, 2006, **90**, 4701–4711.
5 J. Nakanishi, Y. Kikuchi, T. Takarada, H. Nakayama, K. Yamaguchi and M. Maeda, *J. Am. Chem. Soc.*, 2004, **126**, 16314–16315.
6 M. J. Blewitt and R. K. Willits, *Annu. Rev. Biomed. Eng.*, 2007, **35**, 2159–2167.
7 D. R. Albrecht, G. H. Underhill, T. B. Wassermann, R. L. Sah and S. N. Bhatia, *Nat. Methods*, 2006, **3**, 369–375.
8 G. N. Li, L. L. Livi, C. M. Gourd, E. S. Deweerd and D. Hoffman-Kim, *Tissue Eng.*, 2007, **13**, 1035–1047.
9 D. A. Bruzewicz, A. P. McGuigan and G. M. Whitesides, *Lab Chip*, 2008, **8**, 663–671.
10 C. V. Rao, D. M. Wolf and A. P. Arkin, *Nature*, 2002, **420**, 231–237.

11 K. Ino, M. Okochi, N. Konishi, M. Nakatochi, R. Imai, M. Shikida, A. Ito and H. Honda, *Lab Chip*, 2008, **8**, 134–142.
12 N. Q. Balaban, J. Merrin, R. Chait, L. Kowalik and S. Leibler, *Science*, 2004, **305**, 1622–1625.
13 C. M. Nelson, M. M. Vanduijn, J. L. Inman, D. A. Fletcher and M. J. Bissell, *Science*, 2006, **314**, 298–300.
14 A. Khademhosseini, R. Langer, J. Borenstein and J. P. Vacanti, *Proc. Natl. Acad. Sci. USA*, 2006, **103**, 2480–2487.
15 S. V. Graeter, J. H. Huang, N. Perschmann, M. López-García, H. Kessler, J. D. Ding and J. P. Spatz, *Nano Lett.*, 2007, **7**, 1413–1418.
16 S. H. Lee, H. E. Jeong, M. C. Park, J. Y. Hur, H. S. Cho, S. H. Park and K. Y. Suh, *Adv. Mater.*, 2008, **20**, 788–792.
17 K. Johanson, P. L. Allen, R. A. Gonzalez-Villalobos, C. B. Baker, R. D'Elia and T. G. Hammond, *Biotechnol. Bioeng.*, 2006, **93**, 1050–1059.
18 T. Sun, D. Norton, R. J. Mckean, J. W. Haycock, A. J. Ryan and S. Macneil, *Biotechnol. Bioeng.*, 2007, **97**, 1318–1328.
19 V. Ya. Prinz, V. A. Seleznev, A. K. Gutakovsky, A. V. Chehovskiy, V. V. Preobrazhenskii, M. A. Putyato and T. A. Gavrilova, *Physica E*, 2000, **6**, 828–831.
20 O. G. Schmidt and K. Eberl, *Nature*, 2001, **410**, 168.
21 Y. F. Mei, G. S. Huang, A. A. Solovev, E. Bermúdez Ureña, I. Mönch, F. Ding, T. Reindl, R. K. Y. Fu, P. K. Chu and O. G. Schmidt, *Adv. Mater.*, 2008, DOI: 10.1002/adma.200801589.
22 D. J. Thurmer, C. Deneke, Y. F. Mei and O. G. Schmidt, *Appl. Phys. Lett.*, 2006, **89**, 223507.
23 A. Valero, J. N. Post, J. W. van Nieuwkasteele, P. M. ter Braak, W. Kruijer and A. van den Berg, *Lab Chip*, 2008, **8**, 62–67.
24 P. S. Dittrich and A. Manz, *Nat. Rev. Drug Discovery*, 2006, **5**, 210–218.
25 J. C. T. Eijkel and A. van den Berg, *Microfluid. Nanofluid.*, 2005, **1**, 249–267.
26 S. Carnazza, S. Satriano and S. Guglielmino, *J. Phys.: Condens. Matter*, 2006, **18**, S2221–S2230.
27 C. J. Ingham, A. Sprenkels, J. Bomer, D. Molenaar, A. van den Berg, J. E. T. van Hylckama Vlieg and W. M. de Vos, *Proc. Natl. Acad. Sci. USA*, 2007, **104**, 18217–18222.
28 P. S. Dittrich, K. Tachikawa and A. Manz, *Anal. Chem.*, 2006, **78**, 3887–3907.
29 A. Naji and M. F. Harmand, *Biomaterials*, 1991, **12**, 690–694.
30 A. M. Gatti and F. Rivasi, *Biomaterials*, 2002, **23**, 2381–2387.
31 C. Deneke, C. Müller, N. Y. Jin-Phillipp and O. G. Schmidt, *Semicond. Sci. Technol.*, 2002, **17**, 1278–1281.
32 R. Songmuang, C. Deneke and O. G. Schmidt, *Appl. Phys. Lett.*, 2006, **89**, 223109.
33 M. L. Slater, S. O. Sharrow and J. J. Gart, *Proc. Natl. Acad. Sci. USA*, 1977, **74**, 3850–3854.
34 P. G. Lord and A. E. Wheals, *J. Cell Sci.*, 1981, **50**, 361–376.
35 J. Chant and J. R. Pringle, *J. Cell Biol.*, 1995, **129**, 751–765.
36 Y. J. Sheu, Y. Barral and M. Snyder, *Mol. Cell. Biol.*, 2000, **20**, 5235–5247.
37 R. Songmuang, A. Rastelli, S. Mendach and O. G. Schmidt, *Appl. Phys. Lett.*, 2007, **90**, 091905.
38 H. Y. Zhu, I. M. White, J. D. Suter, P. S. Dale and X. D. Fan, *Opt. Express*, 2007, **15**, 9139–9146.

